Micromachined Inverted F Antenna for Integration on Low Resistivity Silicon Substrates

Erik Öjefors, *Student Member, IEEE*, Katia Grenier, *Associate Member, IEEE*, Laurent Mazenq, Fouad Bouchriha, Anders Rydberg, *Member, IEEE*, and Robert Plana, *Member, IEEE*

***Abstract*—This letter addresses the integration of a 24-GHz inverted-F antenna on a low resistivity silicon substrate, using micromachining post-processing techniques compatible with commercial Si/SiGe active device processes. By suspending the radiator on a 2.4 mm^2 large polymer membrane an on-chip antenna with -0.7 dBi gain has been realized.**

***Index Terms*—Antennas, micromachining, silicon.**

I. Introduction

FULLY integrated 24-GHz systems manufactured in commercial silicon-germanium (SiGe) bipolar processes, such as an integrated receiver, have been demonstrated [1]. By monolithically integrating an antenna on chip with such a system, a small, self contained RF module is obtained, which could find applications in short range radar and communication devices operating in the 24-GHz ISM band. Absence of high frequency interconnects and simplified packaging could lead to cost savings. However, in order to achieve the goal of low cost, it is important that the on-chip antenna does not significantly increase the total chip size.

The inverted F antenna (IFA) is a compact antenna type originally proposed for low profile missile antennas [2] which has seen extensive use in mobile communications [3] and has been modified for planar printed circuit board (PCB) implementation in several applications.

Integrated inverted F antennas with good performance have been reported for modified silicon substrates at frequencies up to 20 GHz using proton implantation or silicon-on-quartz [4]. However, such techniques typically require process modifications not available in commercial silicon bipolar and HBT processes. By contrast, low temperature budget bulk micromachining, where selected regions of the lossy substrate is removed, has proved to be a feasible way of post-processing pre-fabricated active device wafers [5].

In this work, we combine the small size of an inverted F antenna with the low losses provided by localized micromachining of the substrate in proximity of the radiator to obtain a compact on chip antenna, compatible with the commonly used low resistivity silicon wafers.

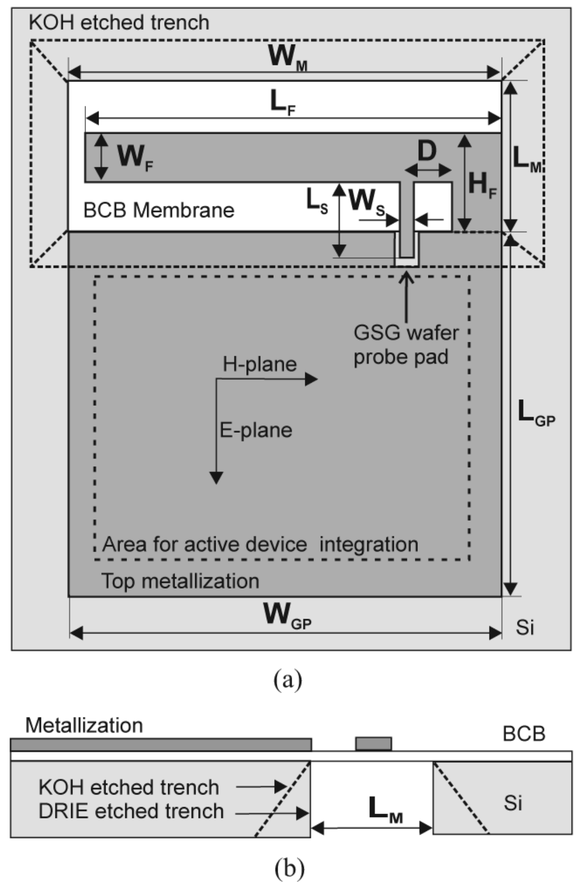

Fig. 1. (a) Top view and (b) cross section of inverted F antenna on micromachined substrate with DRIE (solid line) or KOH (dotted line) etched membrane. Principal E- and H-plane indicated.

II. Design and Simulation

The designed antenna is shown in Fig. 1. The radiator is supported on a 10-μm-thick membrane of low loss ($\varepsilon_r = 2.65$, $\tan\delta = 0.002$) benzocyclobutene (BCB) dielectric [6]. The thin BCB membrane on top of the micromachined substrate provides the radiator with a low effective dielectric constant.

The dimensions of the inverted F section are $W_F = 300$ μm, $L_F = 2500$ μm and $H_F = 580$ μm, thus corresponding to a total radiator length of 3080 μm which is similar to a quarter

Manuscript received March 17, 2005; revised June 2, 2005. This work was supported by the European Commission under the IST-Contracts ARTEMIS and AMICOM. The review of this letter was arranged by Associate Editor J.-G. Ma.

E. Öjefors and A. Rydberg are with the Department of Engineering Sciences, Uppsala University, Uppsala SE-751 20, Sweden (e-mail: erik.ojefors@signal.uu.se).

K. Grenier, L. Mazenq, F. Bouchriha, and R. Plana are with Centre National de la Recherche Scientifique (CNRS), Laboratoire d'Analyse et d'Architecture des Systèmes (LAAS), Toulouse 31077, France.

Digital Object Identifier 10.1109/LMWC.2005.856693

wavelength in free space. As in the case of the inverted-L antenna [7] a larger distance H_F increases the radiation resistance, and thus yields larger bandwidth of the antenna, but also increases the required chip area.

The micromachined membrane is $W_M = 2600\ \mu$m wide, $L_M = 900\ \mu$m long and centered around the F-section of the antenna in order to minimize the dielectric losses of the low resistivity silicon substrate in the region of high electric fields close to the radiator.

The ground-plane has a typical size ($L_{GP} = 2200\ \mu$m, $W_{GP} = 2600\ \mu$m) of a square shaped integrated receiver or transmitter circuit incorporating grounded parts such as ground and power planes. In the simulation it was determined that the majority of the current flows close to the edges, thus not mandating the use of a solid ground-plane.

The distance D between the feed point and the shorting post determines the input impedance at resonance and can thus be selected to provide a suitable value for an active integrated RF-frontend. For characterization purposes a 50-Ω input impedance was selected, requiring a distance $D = 280\ \mu$m between the probe pad and the post. The correct distance was determined by simulation with HFSS [8] using a localized voltage source at the input terminal. The antenna feed consists of a $L_S = 450\ \mu$m long and $W_S = 90\ \mu$m wide conductor which is terminated in a short CPW transmission line, which serves as a probe pad for the ground-signal-ground (GSG) coplanar wafer probe used for the measurements.

The simulated directivity of the antenna at 24.1 GHz is 2.1 dBi with a gain of -0.3 dBi, corresponding to a predicted efficiency of 56% with substrate and metal losses included in the simulation. The principal E- and H-planes of the antenna are indicated in Fig. 1, but due to the asymmetric design of antenna the obtained polarization purity is low.

III. Manufacturing

The antennas were manufactured on 400-μm-thick silicon wafers with 11–15 $\Omega\mathrm{cm}$ bulk resistivity. The wafers were spin-coated with a 10-μm-thick layer of BCB polymer which was cured at a temperature of 250 °C under nitrogen flow. The antenna metallization was deposited on top of the dielectric layer by gold electroplating to a total thickness of 3 μm.

The membranes were released by localized backside etching of the wafer using deep ion reactive etch (DRIE), providing straight walls of the silicon trench as depicted in Fig. 1. A 10-μm -thick photoresist mask was used on the back side of the wafer in order to define the membrane areas.

An additional batch of antennas was processed using potassium hydroxide (KOH) wet chemical etching, yielding slanted walls along the crystal planes of the silicon as indicated by dotted lines in Fig. 1. Silicon nitride, deposited by plasma enhanced chemical vapor deposition (PECVD), was used as mask for the KOH micromachining.

The processed wafers were diced into individual antenna chips of $3.8 \times 3.8\ \mathrm{mm}^2$ size before electrical characterization to prevent substrate coupling to nearby elements on the wafer. No membrane failures have been observed in the preparation or handling of the processed antenna chips.

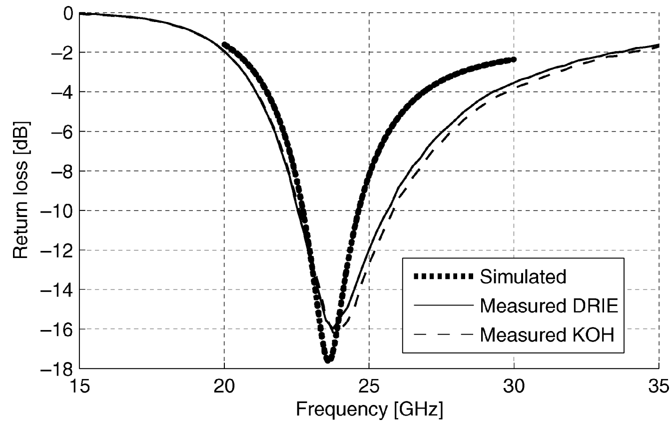

Fig. 2. Measured and simulated return loss for DRIE and KOH etched antennas.

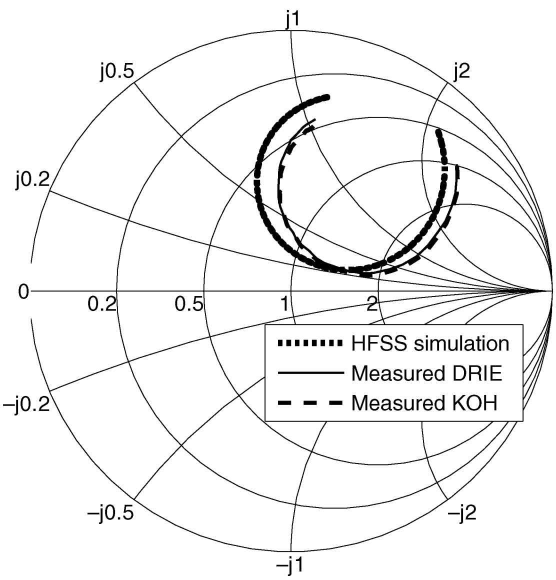

Fig. 3. Measured (DRIE etched solid line, KOH etched dashed) and simulated (dotted line) 20–30 GHz input impedance.

IV. Measurements and Results

The return loss of the on-chip antenna was measured using a wafer probe station which has been modified to prevent reflections from the metallic parts [9]. The antenna under test was mounted on top of a 9-mm-thick styrofoam sheet with $\varepsilon_r = 1$. A microwave absorber was placed beneath the foam sheet to suppress reflections from the metal base plate of the probe station.

The simulated and measured antenna return loss for the designed antennas is plotted in Fig. 2.

The measured return loss agrees with the simulated one with a resonance frequency of 24 GHz and a -10 dB bandwidth of 2 GHz. The larger bandwidth in the measurement can be explained by losses not properly modeled in the simulation and additional radiation losses due to the presence of a wafer probe close to the antenna. Despite the larger amount of silicon removed by the KOH etching method compared to the DRIE one no significant increase in resonance frequency was seen.

The measured input impedance is shown in Fig. 3 together with simulated results obtained with HFSS. The impedance locus does not pass through the 50-Ω point as the original design and feed point selection did not include the effects of chip

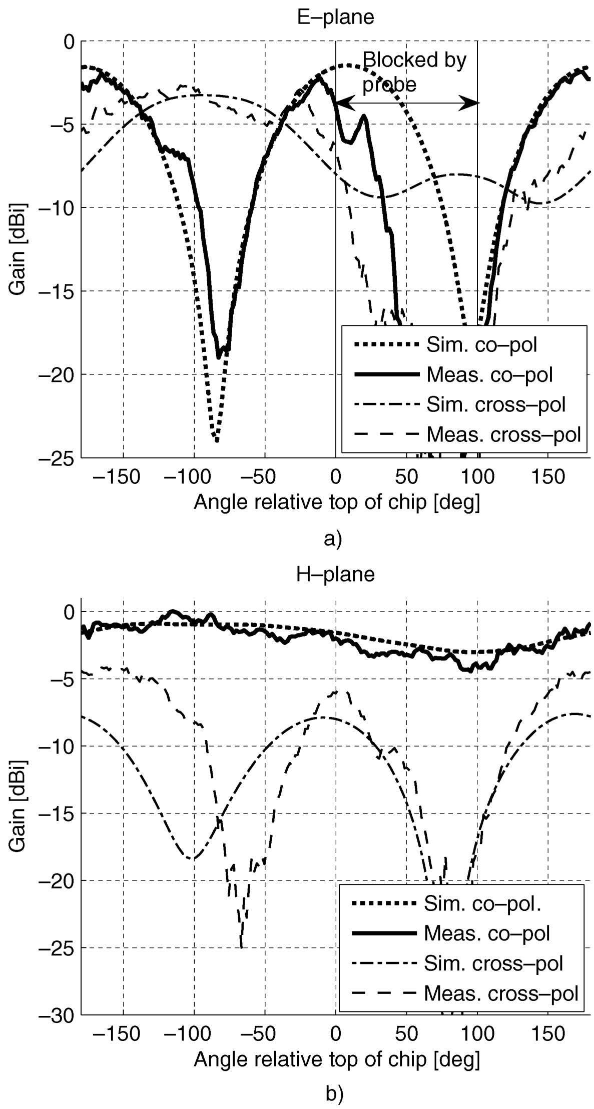

Fig. 4. Simulated and measured co- and cross-polariztion (a) E- and (b) H-plane radiation patterns. 0° in each plane corresponds to the top side of the wafer.

dicing. No differences in antenna impedance were obtained for the DRIE and KOH etched antennas, thus indicating similar radiation and loss resistance.

The antenna radiation pattern was measured in a free space environment with the antenna supported by a 9-mm thick foam sheet. The electrical connection is provided by a wafer probe which partially shadows the antenna in the E-plane. The setup was calibrated for gain measurements using a 20 dBi standard gain horn in place of the antenna under test.

The principal E- and H-plane measured radiation patterns for the DRIE etched antenna are shown in Fig. 4 along with the simulated patterns. A maximum gain of -0.7 dBi was measured at 24.1 GHz. The negative gain, which shows agreement with simulations, is likely caused by dielectric and conductor losses in combination with the low directivity of the antenna.

The E-plane pattern exhibits typical dipole characteristics with nulls at -90 and 90° and maximums in the broadside directions. Good agreement with the simulated results is obtained outside the 0–100° range of angles blocked by the probe setup. The H-plane displays an omnidirectional pattern, closely following the simulated pattern. The increase in cross-polarization visible in both the E-plane and H-plane relative to simulations is likely caused by interaction with the wafer probe, which is positioned in close proximity to the current maximum at the shorting post of the radiator.

V. Conclusion

A micromachined 24-GHz inverted F antenna, with the radiator suspended on a 2.4-mm^2 large micromachined membrane, has been demonstrated on a 15-mm^2 large, low resistivity silicon chip. Due to the use of low temperature post micromachining techniques the demonstrated antenna is suitable for on-chip integration with transceiver circuits manufactured in commercial SiGe HBT and BiCMOS processes. Deep reactive ion etching and KOH wet etching methods for the release of the BCB membrane have been compared with no influence on antenna impedance or tuning seen, despite the different silicon etching profiles obtained. The implemented antenna provides 2-GHz bandwidth at 24 GHz, and a maximum measured gain of -0.7 dBi.

References

[1] E. Sonmez, A. Trasser, K.-B. Schad, P. Abele, and H. Schumacher, "A single-chip 24 GHz receiver front-end using a commercially available SiGe HBT foundry process," in *Proc. IEEE Radio Frequency Integrated Circuits (RFIC) Symp.*, vol. 1, 2002, pp. 159–162.

[2] R. King, C. Harrison, and D. Denton, "Transmission-line missile antennas," *IRE Trans. Antennas Propag.*, vol. 8, no. 1, pp. 88–90, Jan. 1960.

[3] K. Fujimoto and J. R. James, *Mobile Antenna Systems Handbook*, 2nd ed. Norwell, MA: Artech House, 2001.

[4] K. T. Chan, A. Chin, Y. B. Chen, T. S. D. L. Y.-D. Lin, and W. J. Lin, "Integrated antennas on Si, proton-implanted Si and Si-on-quartz," in *IEDM Tech. Dig.*, 2001, pp. 40.6.1–40.6.4.

[5] K. Grenier, D. Dubuc, L. Mazenq, J.-P. Busquere, B. Ducarouge, F. Bouchriha, A. Rennane, V. Lubecke, P. Ancey, and R. Plana, "Polymer based technologies for microwave and millimeterwave applications," in *Proc. IEEE Int. Electron Devices Meeting*, San Francisco, CA, Dec. 2004, pp. 545–548.

[6] *Cyclotene 4046 Data Sheet*, The Dow Chemical Company, Midland, MI.

[7] Z. Chen, "Note on impedance characteristics of L-shaped wire monopole antenna," *Microw. Opt. Technol. Lett.*, vol. 26, no. 1, pp. 22–23, Jul. 2000.

[8] *High-Frequency Structure Simulator (HFSS) Version 5.6, Users Guide*, Agilent Technologies, Palo Alto, CA, 1999.

[9] L. Roy, M. Li, S. Labonte, and N. Simons, "Measurement techniques for integrated-circuit slot antennas," *IEEE Trans. Instrum. Meas.*, vol. 46, no. 4, pp. 1000–1004, Aug. 1997.

射频和天线设计培训课程推荐

易迪拓培训(www.edatop.com)由数名来自于研发第一线的资深工程师发起成立，致力并专注于微波、射频、天线设计研发人才的培养；我们于 2006 年整合合并微波 EDA 网(www.mweda.com)，现已发展成为国内最大的微波射频和天线设计人才培养基地，成功推出多套微波射频以及天线设计经典培训课程和 ADS、HFSS 等专业软件使用培训课程，广受客户好评；并先后与人民邮电出版社、电子工业出版社合作出版了多本专业图书，帮助数万名工程师提升了专业技术能力。客户遍布中兴通讯、研通高频、埃威航电、国人通信等多家国内知名公司，以及台湾工业技术研究院、永业科技、全一电子等多家台湾地区企业。

易迪拓培训课程列表：http://www.edatop.com/peixun/rfe/129.html

射频工程师养成培训课程套装

该套装精选了射频专业基础培训课程、射频仿真设计培训课程和射频电路测量培训课程三个类别共 30 门视频培训课程和 3 本图书教材；旨在引领学员全面学习一个射频工程师需要熟悉、理解和掌握的专业知识和研发设计能力。通过套装的学习，能够让学员完全达到和胜任一个合格的射频工程师的要求…

课程网址：http://www.edatop.com/peixun/rfe/110.html

ADS 学习培训课程套装

该套装是迄今国内最全面、最权威的 ADS 培训教程，共包含 10 门 ADS 学习培训课程。课程是由具有多年 ADS 使用经验的微波射频与通信系统设计领域资深专家讲解，并多结合设计实例，由浅入深、详细而又全面地讲解了 ADS 在微波射频电路设计、通信系统设计和电磁仿真设计方面的内容。能让您在最短的时间内学会使用 ADS，迅速提升个人技术能力，把 ADS 真正应用到实际研发工作中去，成为 ADS 设计专家...

课程网址： http://www.edatop.com/peixun/ads/13.html

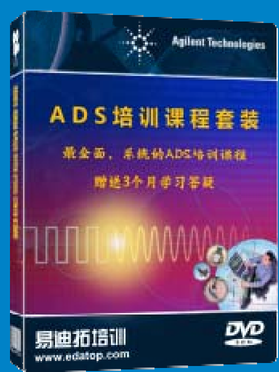

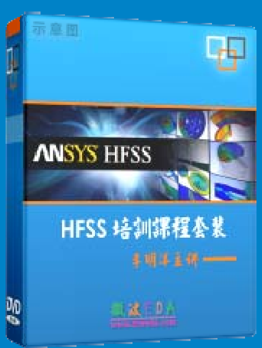

HFSS 学习培训课程套装

该套课程套装包含了本站全部 HFSS 培训课程，是迄今国内最全面、最专业的 HFSS 培训教程套装，可以帮助您从零开始，全面深入学习 HFSS 的各项功能和在多个方面的工程应用。购买套装，更可超值赠送 3 个月免费学习答疑，随时解答您学习过程中遇到的棘手问题，让您的 HFSS 学习更加轻松顺畅…

课程网址：http://www.edatop.com/peixun/hfss/11.html

CST 学习培训课程套装

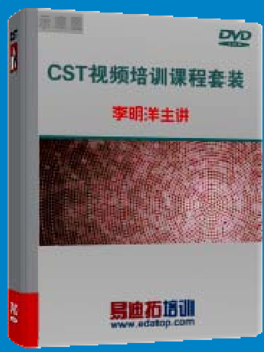

该培训套装由易迪拓培训联合微波 EDA 网共同推出，是最全面、系统、专业的 CST 微波工作室培训课程套装，所有课程都由经验丰富的专家授课，视频教学，可以帮助您从零开始，全面系统地学习 CST 微波工作的各项功能及其在微波射频、天线设计等领域的设计应用。且购买该套装，还可超值赠送 3 个月免费学习答疑…

课程网址：http://www.edatop.com/peixun/cst/24.html

HFSS 天线设计培训课程套装

套装包含 6 门视频课程和 1 本图书，课程从基础讲起，内容由浅入深，理论介绍和实际操作讲解相结合，全面系统的讲解了 HFSS 天线设计的全过程。是国内最全面、最专业的 HFSS 天线设计课程，可以帮助您快速学习掌握如何使用 HFSS 设计天线，让天线设计不再难…

课程网址：http://www.edatop.com/peixun/hfss/122.html

13.56MHz NFC/RFID 线圈天线设计培训课程套装

套装包含 4 门视频培训课程，培训将 13.56MHz 线圈天线设计原理和仿真设计实践相结合，全面系统地讲解了 13.56MHz 线圈天线的工作原理、设计方法、设计考量以及使用 HFSS 和 CST 仿真分析线圈天线的具体操作，同时还介绍了 13.56MHz 线圈天线匹配电路的设计和调试。通过该套课程的学习，可以帮助您快速学习掌握 13.56MHz 线圈天线及其匹配电路的原理、设计和调试…

详情浏览：http://www.edatop.com/peixun/antenna/116.html

我们的课程优势：

※ 成立于 2004 年，10 多年丰富的行业经验，

※ 一直致力并专注于微波射频和天线设计工程师的培养，更了解该行业对人才的要求

※ 经验丰富的一线资深工程师讲授，结合实际工程案例，直观、实用、易学

联系我们：

※ 易迪拓培训官网：http://www.edatop.com

※ 微波 EDA 网：http://www.mweda.com

※ 官方淘宝店：http://shop36920890.taobao.com